Water Storage, Net Precipitation, and Evapotranspiration in the Mackenzie River Basin from October 2002 to September 2009 Inferred from GRACE Satellite Gravity Data

E. MORROW AND J. X. MITROVICA

Department of Earth and Planetary Sciences, Harvard University, Cambridge, Massachusetts

G. FOTOPOULOS

Department of Geosciences, The University of Texas at Dallas, Dallas, Texas

(Manuscript received 4 February 2010, in final form 5 November 2010)

ABSTRACT

Gravity Recovery and Climate Experiment (GRACE) satellite gravity data are used to determine the variability of terrestrial water storage within the Mackenzie River basin from October 2002 to September 2009. During that period, it is estimated that there is no significant (7 yr) linear trend in the water storage after having accounted for postglacial rebound using the ICE-5G (VM2) ice sheet and Earth viscosity model. Errors in this model may alter this conclusion. The GRACE gravity data are also combined with precipitation and river discharge datasets to estimate trends in net precipitation and evapotranspiration in the basin. Net precipitation is seen to have a significant trend with a corresponding increase in river discharge. Evapotranspiration was found to be constant over the study period.

1. Introduction

The Mackenzie River basin (MRB) is the second largest basin in North America, with a drainage area of about 1.8×10^6 km^2, and is the largest basin on the continent to drain freshwater into the Arctic Ocean (Woo and Thorne 2003). Freshwater discharge affects the salinity of the Arctic Ocean (Macdonald et al. 1999) and in turn the Atlantic meridional overturning circulation (Broecker 1997). Partly because of this connection to the global climate system, the overall hydrological cycle of the region and its elements have been the subject of numerous studies (e.g., Bjornsson et al. 1995; Louie et al. 2002; Serreze et al. 2003). A particularly comprehensive analysis was the Water and Energy Budget Study (WEBS; Szeto et al. 2008) associated with the Mackenzie Global Energy and Water Cycle Experiment (GEWEX) Study (MAGS; Stewart et al. 1998; Rouse et al. 2003). The MAGS WEBS combined models, in situ observations, and remotely sensed datasets to formulate a complete water and energy budget of the MRB. However, because of the difficulties in measuring soil moisture and evapotranspiration and the scarcity of observations on a regional scale, both of these parameters were estimated from forecast models (Szeto et al. 2008). The Gravity Recovery and Climate Experiment (GRACE) represents a unique opportunity for estimating terrestrial water storage (TWS) and, when river discharge and precipitation datasets exist, inferring evapotranspiration.

Monthly GRACE gravity field estimates have been used to determine the time variability of surface-mass anomalies (e.g., Swenson and Wahr 2002; Wahr et al. 2004) since the twin satellites were launched in 2002. These surface-mass anomalies have been used to derive estimates of the TWS in continental hydrological cycles over both global and regional scales (e.g., Tapley et al. 2004; Syed et al. 2005; Crowley et al. 2006; Syed et al. 2008). Studies have also combined GRACE-determined TWS with precipitation and river discharge datasets to estimate evapotranspiration in many major drainage basins, though not the Mackenzie (Ramillien et al. 2006; Rodell et al. 2004; Swenson and Wahr 2006). Our work complements previous model-based studies of the Mackenzie region (e.g., Stewart et al. 1998; Rouse et al. 2003) by contributing estimates and trends of net precipitation and evapotranspiration derived from GRACE-inferred water storage, river discharge measurements, and precipitation datasets.

Corresponding author address: E. Morrow, Department of Earth and Planetary Sciences, Harvard University, 20 Oxford Street, Cambridge, MA 02138.
E-mail: emorrow@fas.harvard.edu

DOI: 10.1175/2010JHM1278.1

© 2011 American Meteorological Society

Unauthenticated | Downloaded 07/29/21 12:24 AM UTC

We first use GRACE data to estimate the variability of the terrestrial water storage in the MRB. The estimate is then combined with river discharge measurements to estimate the net precipitation in the basin. We then estimate the (7 yr) trend of the basin evapotranspiration by combining the storage variation with regional precipitation and river discharge observations. The results are then compared with evapotranspiration time series estimated from the Global Land Data Assimilation System (GLDAS) driving the Noah, Variable Infiltration Capacity (VIC), Mosaic, and Community Land Model (CLM) land surface models (LSMs).

2. Terrestrial water storage

The present analysis used the Center for Space Research Release 4 (CSR RL04) spherical harmonic solutions for every month from October 2002 to September 2009 with the exception of June 2003, which was not in the available dataset. The RL04 datasets contain harmonics up to degree 60, which roughly corresponds to a half-wavelength of 330 km. A decorrelation filter (Chambers 2006) was applied to the spherical harmonic coefficients to correct for high-order correlated errors (Swenson and Wahr 2006). Since the MRB is located in the North American Arctic, the change in gravity field within the basin can be attributed to both water storage and slow adjustments associated with ongoing postglacial rebound (PGR) (Tamisiea et al. 2005). To isolate the geoid variability due to water storage from that due to postglacial rebound, the latter was subtracted from observed GRACE signals by using a numerical prediction based on the ICE-5G (VM2) ice sheet and Earth viscosity model (Peltier 2004). To determine the anomalous geoid variability, the spherical harmonics (after correction for postglacial rebound) were averaged over all 83 monthly GRACE solutions, and the average was removed from each coefficient set. The anomaly coefficients were then converted into equivalent surface water depth (ESWD) using the Love number methodology described in Swenson and Wahr (2002).

To generate a regional average of the anomalous surface mass, a mask defining the MRB was constructed (i.e., a field equal to one in the MRB and zero elsewhere). The mask/MRB has maximum north–south and east–west dimensions of 1500 and 1400 km, respectively. A Gaussian smoothing function with a half-width radius of 350 km was applied to the mask to reduce the errors associated with the higher-order harmonics. Figure 1 shows the averaging function constructed in this manner. The 350-km half-width radius was selected as a trade-off between estimation error and leakage of

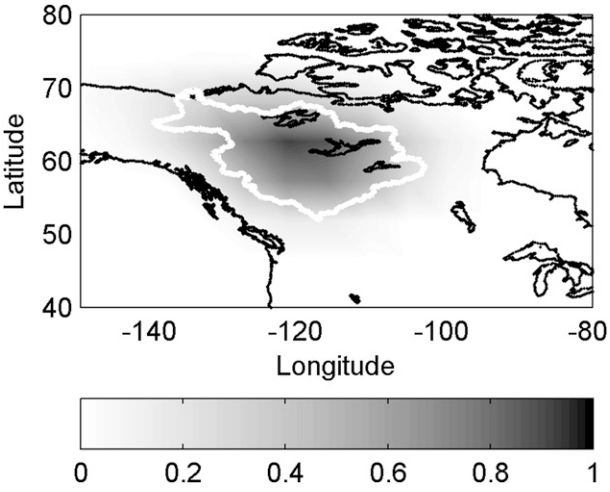

FIG. 1. Averaging mask used for the MRB. The shading indicates the averaging weight associated with a Gaussian smoothing function with a half-width of 350 km.

the averaging into regions outside the mask (Swenson and Wahr 2002; Tapley et al. 2004). This half-width also closely corresponds to the maximum resolution available from a spherical harmonic representation to degree 60 (Rummel et al. 2002). Spectral leakage from the Gaussian filter causes an attenuation of trends in the basin average. To account for this attenuation, a filtered basin average was computed for the case of a synthetic, constant signal, and this was compared with the associated, unfiltered basin average. Specifically, the ratio between the unfiltered and filtered averages yielded a scaling factor of 1.25 that was applied to every subsequent filtered average to account for the signal leakage from the basin.

Signal leakage into the MRB from influences outside the basin is also a concern, particularly given the proximity to melting Alaskan glaciers. To account for this leakage, spatially localized mass loss trends in the Alaskan glaciers from 1993 to 2007 (G. Cogley 2010, personal communication) were filtered using the Gaussian kernel and scaled to account for filter attenuation. The melting glaciers contributed a trend of -0.009 mm day^{-1} to the MRB signal, which was consequently removed from the storage trends.

The degree-2 coefficients in the GRACE spherical harmonics are characterized by a large uncertainty (Velicogna and Wahr 2005). In this regard, following Velicogna and Wahr (2005), these coefficients were replaced by the degree-two coefficients determined from satellite laser ranging, as analyzed by Cheng and Tapley (2004).

The errors in the ESWD were estimated from a Monte Carlo analysis that perturbed the spherical harmonic

Unauthenticated | Downloaded 07/29/21 12:24 AM UTC

coefficients with their associated error statistics. The mean and standard deviation of the perturbation results for each of the monthly ESWD estimates were then calculated. This error estimation was performed prior to filtering the spherical harmonics, thus enabling the use of the error statistics provided with the GRACE dataset. An unweighted Levenberg–Marquardt least squares regression was performed on the ESWD (W) to a form that contains constant (W_0), linear (W_1), quadratic (W_2) and periodic (W^*) terms as follows:

$$W(t) = W_0 + W_1 t + W_2 t^2 + W^*(t), \qquad (1)$$

where t is the time referenced to an arbitrary epoch and $W^*(t)$ is represented by the summation of four sinusoidal terms that each contain independent amplitude, frequency, and phase parameters that were included as state variables in the nonlinear curve fit procedure. The regression found the optimal period of the sinusoidal terms to be 18, 27, 232, and 312 days.

The four sinusoidal terms were included in the least squares fit to add additional degrees of freedom to the system for a better accounting of the higher-order variability than is achieved by either a simple polynomial fit or by using two sinusoids representing the annual and semiannual signals. The use of four sinusoids reduced the root-mean square of the postfit residuals by 61% relative to a fit to annual and semiannual terms and was consequently deemed a better representation of the higher-order variability.

Figure 2 shows the monthly estimates for W in the MRB determined from GRACE data (circles) along with the least squares fit (solid line) and the linear and quadratic trend within this fit (dashed line). Table 1 lists the coefficients determined from the least squares curve fit. The water storage is characterized by insignificant linear and quadratic trends of -0.002 ± 0.012 mm day^{-1} and -0.0002 ± 0.0017 mm day^{-1} year^{-1}, respectively.

Ongoing postglacial rebound is a significant component of the secular trend in the gravity signal within the MRB, and our correction for this effect, based on the ICE-5G (VM2) model, is susceptible to two classes of error. First, the ICE-5G (VM2) model is composed of both an ice sheet history and a one-dimensional (depth dependent) mantle viscosity profile; predictions based on this model are highly sensitive to errors in each of these elements of the model. Second, ICE-5G (VM2) is constrained to gravimetric observations (Peltier 2004) that contain hydrological as well as PGR signals, and so the adoption of this model to correct for the latter may introduce a bias in the PGR-corrected GRACE trends. In the following, we attempt to estimate the size of both these errors.

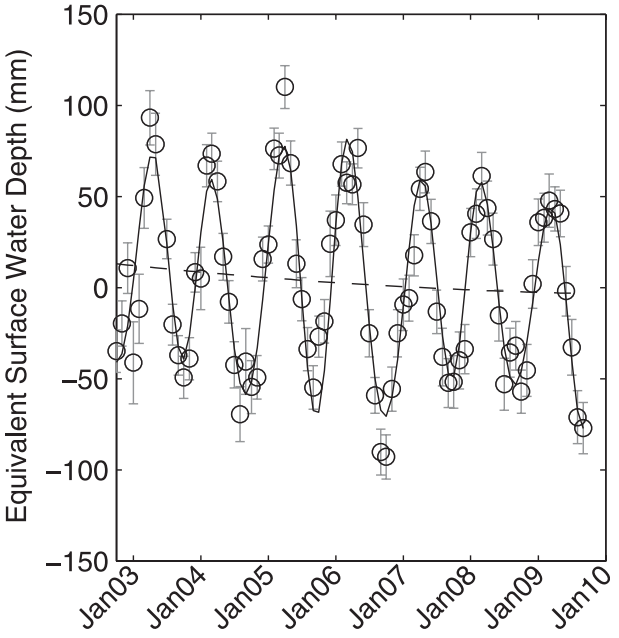

FIG. 2. ESWD anomalies in the MRB inferred from GRACE data (circles) and a least squares line of best fit to this data [solid line; Eq. (1)]. The net linear and quadratic trend of the least squares fit is shown as the dashed line (the coefficients of the trend are listed in Table 1).

Figure 3 shows the GRACE-derived water storage time series for cases where the signal is not corrected for postglacial rebound, as well as after a correction has been applied using the ICE-5G (VM2) model (as in Fig. 2) and the older ICE-3G model (Tushingham and Peltier 1991). In contrast to ICE-5G, ICE-3G was derived without an assimilation of gravity observations. It is clear from the figure that the uncorrected storage has a significant positive trend, which the ICE-5G correction (0.055 mm day^{-1} in equivalent surface water depth) effectively removes. In contrast, the ICE-3G correction has a smaller amplitude (0.020 mm day^{-1}), leading to a significant residual (PGR corrected) trend.

To isolate the degree to which the hydrological signal is contaminating the gravimetric constraints used in the original derivation of the ICE-5G (VM2) model, we use the 1.0° GLDAS/Noah model output to estimate the time variation of the water storage at the closest constraint point to the Mackenzie River basin, located at Churchill, Manitoba. The gravimetric constraint on the

TABLE 1. TWS least squares fit coefficients.

Least squares fit coefficient	Value
Constant (mm) (W_0)	13 ± 7
Linear (mm day^{-1}) (W_1)	-0.002 ± 0.012
Quadratic (mm day^{-1} yr^{-1}) (W_2)	0.0001 ± 0.0017

Unauthenticated | Downloaded 07/29/21 12:24 AM UTC

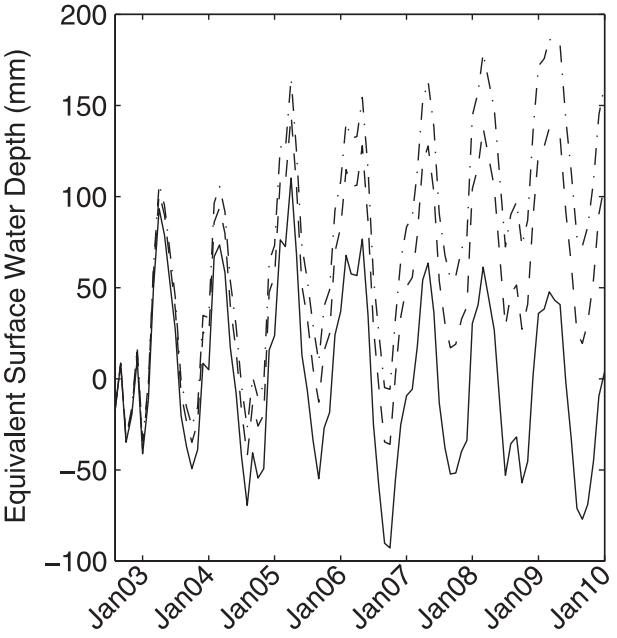

FIG. 3. Water storage time series with no postglacial signal removed (dotted–dashed line), an ICE-3G-based correction (dashed line), and an ICE-5G-based correction (solid line).

ICE-5G (VM2) model at this site was associated with measurements by Lambert et al. (2001), who obtained a gravity anomaly at the earth's solid surface of -2.13 ± 0.23 μGal yr^{-1}. Converting a least squares fit of the GLDAS water storage into an equivalent gravity anomaly yielded a water storage contribution of -0.20 ± 0.08 μGal yr^{-1} at this site. It should be noted that in using the results of the GLDAS/Noah land surface model to estimate the hydrological component of the gravity anomaly that such models are known to be less accurate in snow-dominated/glaciated regions due to snow or missing surface or groundwater components. Nevertheless, while the GLDAS-derived hydrological gravity component falls within the experimental error, it still comprises 10% of the gravity observation, a portion that could impact any PGR-corrected linear trends extracted from the water storage signal.

In the analyses below, we use the ICE-5G (VM2) model to correct the GRACE time series; however, we emphasize that the accuracy of our estimates of various hydrological trends will dependent on the veracity of the ICE-5G (VM2) ice history and earth model.

3. Linear trends in net precipitation

Trends in the difference between precipitation (P) and evapotranspiration (E), also called net precipitation, are important because they describe changes to the moisture flux between the land surface and the atmosphere. Changes in this flux affect local atmospheric moisture content, and this has implications for regional climate because of the strength of water vapor as a greenhouse gas. Estimates of $P - E$ can be derived from the following terrestrial hydrological balance (e.g. Crowley et al. 2006):

$$\frac{dW(t)}{dt} = P(t) - R(t) - E(t), \tag{2}$$

where R is the runoff within the basin.

Investigating the hydrological cycle in more detail, the terms on the right-hand side (rhs) of Eq. (2) were divided into periodic and nonperiodic constituents as was done for the water storage in Eq. (2). As an example, following Crowley et al. (2006), the discharge can be expanded into constant, linear, and periodic terms as

$$R(t) = R_0 + R_1 t + R^*(t) \tag{3}$$

and similar equations may be written for $P - E$. As in the case of the water storage representation, $R^*(t)$ was represented as the summation of four sinusoidal terms with the same frequencies as were derived in the water storage decomposition.

The basin runoff was constrained using data from a flow gauge (station 10LC014) maintained by the Water Survey of Canada on the Mackenzie River at Arctic Red River. While this gauge only represents drainage from 1.68×10^6 km^2 of the 1.8×10^6 km^2 area of the entire basin, it is the last gauge before the river distributes itself into the Mackenzie delta and as such is a good approximation for the total flow for the Mackenzie River system (Woo and Thorne 2003). The river discharge data were evenly distributed over the basin, and the same 350-km half-width Gaussian smoothing filter was applied to this distribution. Table 2 includes a summary of the least squares fit to the river discharge (plotted with the original time series in Fig. 4), which indicates an increase in the discharge rate over the study period.

TABLE 2. Precipitation and discharge flux least squares fit coefficients.

Least squares fit coefficient	Value
P constant (mm day^{-1}) (P_0)	1.42 ± 0.07
P linear (mm day^{-1} yr^{-1}) (P_1)	0.011 ± 0.016
R constant (mm day^{-1}) (R_0)	0.35 ± 0.01
R linear (mm day^{-1} yr^{-1}) (R_1)	0.013 ± 0.004

To estimate the linear trend in net precipitation, Eq. (1) was differentiated with respect to time and substituted into Eq. (2), along with the decomposed versions of $P - E$ and R. Neglecting the periodic components and

Unauthenticated | Downloaded 07/29/21 12:24 AM UTC

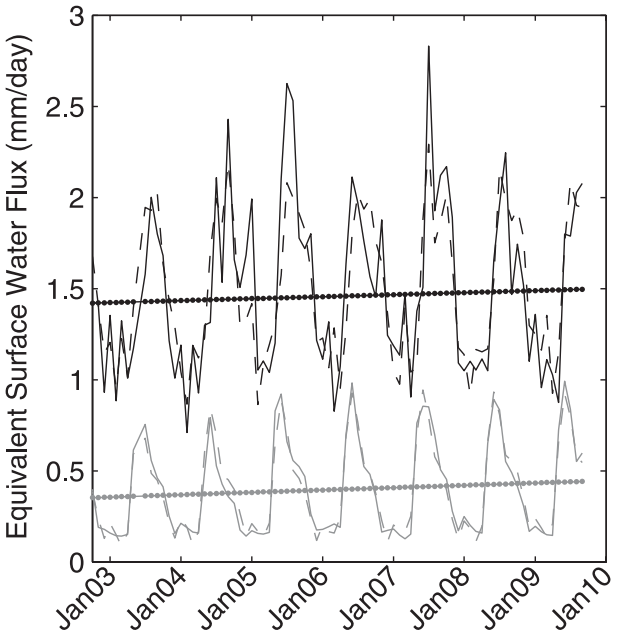

FIG. 4. Precipitation within, and Mackenzie River discharge from, the MRB. The solid black line is the precipitation rate inferred from CMAP, the dashed black line is the curve fit to the precipitation rate, and the dotted black line is the linear trend of this precipitation. The solid gray line is the discharge from the Mackenzie River, the dashed gray line is the curve fit to the discharge, and the dotted gray line is the linear trend of the river discharge.

collecting terms of similar order in t and t^2 yields two equations as follows:

$$(P - E)_0 = R_0 + W_1,$$
$$(P - E)_1 = R_1 + 2W_2. \quad (4)$$

Performing this calculation indicates that annual net precipitation over the study period was 0.35 ± 0.11 mm day^{-1} with a rate of change of 0.013 ± 0.006 mm day^{-1} yr^{-1}. This equates to an annual average moisture addition of 132 ± 42 mm to the basin, which agrees well with the estimate from Serreze et al. (2003) of 142 mm. Table 3 summarizes the calculation results. The linear trend is significantly larger than the Arctic Climate Impact Assessment projections of an increase in net precipitation over the Mackenzie River basin of 10% from 1981 to 2000 to 2071 to 2090 (Walsh et al. 2005). However, the short duration of the GRACE dataset, and the potential errors in the ICE-5G (VM2) model, means that this discrepancy may not be significant.

As first discussed by Rodell et al. (2004), care must be exercised when combining temporally averaged GRACE data products with other hydrological datasets using the instantaneous water balance relation [Eq. (2)]. Swenson and Wahr (2006) demonstrate that a full accounting of the relationship between the GRACE-estimated monthly storage changes and the other hydrological fluxes [i.e., the left-hand side of Eq. (2)] requires a term representing the total flux accumulation rate from one GRACE averaging period to another and a second term representing the difference in the average flux accumulation between the GRACE period and the previous one divided by the time interval between the start of the first averaging period to the beginning of the second. However, to allow for the computation of the monthly averages of the $P - E$ flux (and later the E flux), the full relationship is approximated by the average accumulation rate from one GRACE period to another. To estimate the error incurred by this approximation, the root-mean-squared values of the approximate and full flux accountings were computed over the study period using the Climate Prediction Center (CPC) Merged Analysis of Precipitation (CMAP), Water Survey of Canada discharge, and GLDAS/Noah evapotranspiration estimates. A comparison of the root-mean-squared values indicates that the approximation introduces a 30% error into the flux estimate that is added in quadrature to the error on the $P - E$ (and E) estimates.

4. Linear trends in evapotranspiration

To further explore relative contributions to the hydrological balance, we add precipitation estimates to Eq. (2) to compare observed trends in precipitation with estimates of evapotranspiration.

The precipitation in the MRB was determined using the mean monthly precipitation rates provided by the CMAP datasets on a 2.5° × 2.5° global grid. To perform a consistent comparison with the water storage, the precipitation dataset was processed with the same 350-km half-width Gaussian smoothing filter that was previously

TABLE 3. Net precipitation and evapotranspiration linear trend estimates (N/A = not available).

Trend coefficient	Estimated value	GLDAS value
Net precipitation constant (mm day^{-1}) [$(P - E)_0$]	0.35 ± 0.11	N/A
Net precipitation linear (mm day^{-1} yr^{-1}) [$(P - E)_1$]	0.013 ± 0.006	N/A
E constant (mm day^{-1}) (E_0)	1.07 ± 0.33	0.84 ± 0.19
E linear (mm day^{-1} yr^{-1}) (E_1)	−0.002 ± 0.017	0.014 ± 0.004

Unauthenticated | Downloaded 07/29/21 12:24 AM UTC

applied to the GRACE dataset. The results of the least squares fit to the precipitation time series shown in Fig. 4 and summarized in Table 2 indicate an increasing trend in the precipitation over the study period.

To estimate the linear trend in evapotranspiration, we rearrange Eq. (4) to give

$$E_0 = P_0 - R_0 - W_1,$$
$$E_1 = P_1 - R_1 - 2W_2. \quad (5)$$

Each of the terms on the rhs is determined from the results of the least squares fits on P, R, and W. Table 3 summarizes the results of this exercise. The table also includes the analogous values determined from the mean and standard deviation of trends fit to the evapotranspiration time series of the four land surface models associated with GLDAS: Noah, VIC, CLM, and Mosaic. There is clearly excellent agreement between the constant rate values of these two estimates. The GLDAS linear trend in E is greater than the estimated balance value; however, the discrepancy is insignificant relative to the error associated with these estimates.

The GEWEX study compared the basin-averaged evapotranspiration estimates of five models and found an average of 1.12 mm day^{-1} with a standard deviation of 0.38 mm day^{-1} over the 5-yr analysis period that spanned from June 1997 to May 2002 (Szeto et al. 2008). Our estimate of 1.07 ± 0.33 mm day^{-1} agrees well with the GEWEX results. The GEWEX study does not present a trend in the evapotranspiration.

The separation of the balance components indicates that evapotranspiration is the largest hydrological sink in the basin, with a rate that is greater than 3 times that of the river discharge. However, the associated trends suggest that the discharge rate is increasing significantly faster than changes in evapotranspiration rate. The implication of the river discharge becoming a stronger sink relative to the evapotranspiration is that freshwater input to the Arctic Ocean will be greater than if evapotranspiration remains the dominant sink because of precipitation recycling on land. The increases to freshwater discharge may have consequences for climate, as discussed above.

5. Summary

GRACE provides a powerful means of estimating regional terrestrial water storage in large basins. We use GRACE data in combination with the ICE-5G (VM2) model to infer that there was no statistically significant trend in water storage within the MRB, the largest North American river system flowing into the Arctic Ocean, between October 2002 and September 2009. However, we caution that errors in the ICE-5G model may alter this conclusion. Moreover, by combining the water storage estimate with precipitation and river discharge observations, the (7 yr) linear trends of net precipitation and evapotranspiration were also estimated for the MRB. Net precipitation was found to have an increasing trend that is significantly larger than the model-derived predictions appearing in the Arctic Climate Impact Assessment report.

No significant increase in evapotranspiration was found over the study period with the result that the precipitation was absorbed by a comparable increase in river discharge. The constant component of evapotranspiration, E_0, is in good agreement with both the GLDAS-associated land surface models and other previous (non-GRACE) studies of the basin hydrology. However, our first-order component to the linear trend is smaller than the model-estimated value, though the large error associated with both the GLDAS output value and the balance value makes the discrepancy insignificant.

We emphasize that all of the above-mentioned results are based on a relatively limited (7 yr) GRACE time window and that these estimates may be biased by the adopted postglacial rebound model. Our conclusions are, in this regard, preliminary. Nevertheless, our results suggest that continued monitoring of the hydrological trends is in order, and in this case the methodology we outline above should serve as a framework for such analyses.

Acknowledgments. The authors thank three anonymous reviewers for their useful advice in improving the manuscript. The authors also thank Graham Cogley for providing the Alaskan glacier mass loss trend data. CMAP precipitation data were provided by the NOAA/OAR/ESRL PSD in Boulder, Colorado, via its Web site (available at http://www.cdc.noaa.gov). GLDAS data used in this study were acquired as part of the mission of NASA's Earth Science Division and archived and distributed by the Goddard Earth Science Data and Information Services Center.

REFERENCES

Bjornsson, H., L. A. Mysak, and R. D. Brown, 1995: On the interannual variability of precipitation and runoff in the Mackenzie drainage basin. *Climate Dyn.,* **12,** 67–76.

Broecker, W. S., 1997: Thermohaline circulation, the Achilles heel of our climate system: Will man-made CO_2 upset the current balance? *Science,* **278,** 1582–1588, doi:10.1126/science.278.5343.1582.

Chambers, D. P., 2006: Evaluation of new GRACE time-variable gravity data over the ocean. *Geophys. Res. Lett.,* **33,** L17603, doi:10.1029/2006GL027296.

Unauthenticated | Downloaded 07/29/21 12:24 AM UTC

Cheng, M., and B. D. Tapley, 2004: Variations in the earth's oblateness during the past 28 years. *J. Geophys. Res.,* **109,** B09402, doi:10.1029/2004JB003028.

Crowley, J. W., J. X. Mitrovica, R. C. Bailey, M. E. Tamisiea, and J. L. Davis, 2006: Land water storage within the Congo basin inferred from GRACE satellite gravity data. *Geophys. Res. Lett.,* **33,** L19402, doi:10.1029/2006GL027070.

Lambert, A., N. Courtier, G. S. Sasagawa, F. Klopping, D. Winester, T. S. James, and J. O. Liard, 2001: New constraints on Laurentide postglacial rebound from absolute gravity measurements. *Geophys. Res. Lett.,* **28,** 2109–2112.

Louie, P. Y. T., W. D. Hogg, M. D. MacKay, X. Zhang, and R. F. Hopkinson, 2002: The water balance climatology of the Mackenzie basin with reference to the 1994/95 water year. *Atmos.–Ocean,* **40,** 159–180.

Macdonald, R. W., E. C. Carmack, F. A. McLaughlin, K. K. Falkner, and J. H. Swift, 1999: Connections among ice, runoff and atmospheric forcing in the Beaufort gyre. *Geophys. Res. Lett.,* **26,** 2223–2226.

Peltier, W. R., 2004: Global glacial isostasy and the surface of the ice-age earth: The ICE-5G (VM2) model and GRACE. *Annu. Rev. Earth Planet. Sci.,* **32,** 111–149, doi:10.1146/annurev.earth.32.082503.144359.

Ramillien, G., F. Frappart, A. Güntner, T. Ngo-Duc, A. Cazenave, and K. Laval, 2006: Time variations of the regional evapotranspiration rate from Gravity Recovery and Climate Experiment (GRACE) satellite gravimetry. *Water Resour. Res.,* **42,** W10403, doi:10.1029/2005WR004331.

Rodell, M., J. S. Famiglietti, J. Chen, S. I. Seneviratne, P. Viterbo, S. Holl, and C. R. Wilson, 2004: Basin scale estimates of evapotranspiration using GRACE and other observations. *Geophys. Res. Lett.,* **31,** L20504, doi:10.1029/2004GL020873.

Rouse, W. R., and Coauthors, 2003: Energy and water cycles in a high-latitude, north-flowing river system: Summary of results from the Mackenzie GEWEX study—Phase 1. *Bull. Amer. Meteor. Soc.,* **84,** 73–87.

Rummel, R., G. Balmino, J. Johannessen, P. Visser, and P. Woodworth, 2002: Dedicated gravity field missions—Principles and aims. *J. Geodyn.,* **33,** 3–20.

Serreze, M. C., D. H. Bromwich, M. P. Clark, A. J. Etringer, T. Zhang, and R. Lammers, 2003: Large-scale hydroclimatology of the terrestrial Arctic drainage system. *J. Geophys. Res.,* **108,** 8160, doi:10.1029/2001JD000919.

Stewart, R. E., and Coauthors, 1998: The Mackenzie GEWEX Study: The water and energy cycles of a major North American river basin. *Bull. Amer. Meteor. Soc.,* **79,** 2665–2683.

Swenson, S., and J. Wahr, 2002: Estimated effects of the vertical structure of atmospheric mass on the time-variable geoid. *J. Geophys. Res.,* **107,** 2194, doi:10.1029/2000JB000024.

——, and ——, 2006: Estimating large-scale precipitation minus evapotranspiration from GRACE satellite gravity measurements. *J. Hydrometeor.,* **7,** 252–270.

Syed, T. H., J. S. Famiglietti, J. Chen, M. Rodell, S. I. Seneviratne, P. Viterbo, and C. R. Wilson, 2005: Total basin discharge for the Amazon and Mississippi River basins from GRACE and a land-atmosphere water balance. *Geophys. Res. Lett.,* **32,** L24404, doi:10.1029/2005GL024851.

——, ——, M. Rodell, J. Chen, and C. R. Wilson, 2008: Analysis of terrestrial water storage changes from GRACE and GLDAS. *Water Resour. Res.,* **44,** W02433, doi:10.1029/2006WR005779.

Szeto, K. K., H. Tran, M. D. MacKay, and R. Crawford, 2008: The MAGS Water and Energy Budget Study. *J. Hydrometeor.,* **9,** 96–115.

Tamisiea, M. E., E. W. Leuliette, J. L. Davis, and J. X. Mitrovica, 2005: Constraining hydrological and cryospheric mass flux in southeastern Alaska using space-based gravity measurements. *Geophys. Res. Lett.,* **32,** L20501, doi:10.1029/2005GL023961.

Tapley, B. D., S. Bettadpur, J. C. Ries, P. F. Thompson, and M. M. Watkins, 2004: GRACE measurements of mass variability in the earth system. *Science,* **305,** 503–505, doi:10.1126/science.1099192.

Tushingham, A. M., and W. R. Peltier, 1991: ICE-3G: A new global model of late Pleistocene deglaciation based upon geophysical predictions of post-glacial relative sea level change. *J. Geophys. Res.,* **96,** 4497–4523.

Velicogna, I., and J. Wahr, 2005: Greenland mass balance from GRACE. *Geophys. Res. Lett.,* **32,** L18505, doi:10.1029/2005GL023955.

Wahr, J., S. Swenson, V. Zlotnicki, and I. Velicogna, 2004: Time-variable gravity from GRACE: First results. *Geophys. Res. Lett.,* **31,** L11501, doi:10.1029/2004GL019779.

Walsh, J. E., and Coauthors, 2005: Cryosphere and hydrology. *Arctic Climate Impact Assessment: Scientific Report,* C. Symon, L. Arris, and B. Heal, Eds., Cambridge University Press, 183–242.

Woo, M. K., and R. Thorne, 2003: Streamflow in the Mackenzie basin, Canada. *Arctic,* **56,** 328–340.

Unauthenticated | Downloaded 07/29/21 12:24 AM UTC